

Raman spectra of R₂O₃ (R—rare earth) sesquioxides with C-type bixbyite crystal structure: A comparative study

M. V. Abrashev, N. D. Todorov, and J. Geshev

Citation: *Journal of Applied Physics* **116**, 103508 (2014); doi: 10.1063/1.4894775

View online: <http://dx.doi.org/10.1063/1.4894775>

View Table of Contents: <http://scitation.aip.org/content/aip/journal/jap/116/10?ver=pdfcov>

Published by the *AIP Publishing*

Articles you may be interested in

[IUPAC-NIST Solubility Data Series. 94. Rare Earth Metal Iodides and Bromides in Water and Aqueous Systems. Part 2. Bromides](#)

J. Phys. Chem. Ref. Data **42**, 013101 (2013); 10.1063/1.4766752

[The peculiar magnetic property evolution along RCu₃Mn₄O₁₂ \(R = Y, La, Pr, Nd, Sm, Eu, Gd, Tb, Dy, Ho, Er, Tm, Yb, and Lu\): A first-principles study](#)

Appl. Phys. Lett. **97**, 232504 (2010); 10.1063/1.3524527

[Correlation of structural distortion with magnetic properties in electron-doped Ca_{0.9}R_{0.1}MnO₃ perovskites \(R = rare-earth\)](#)

J. Appl. Phys. **108**, 063928 (2010); 10.1063/1.3481419

[Magnetolectric and magnetoelastic properties of rare-earth ferroborates](#)

Low Temp. Phys. **36**, 511 (2010); 10.1063/1.3457390

[Dielectric and optical properties of epitaxial rare-earth scandate films and their crystallization behavior](#)

Appl. Phys. Lett. **88**, 262906 (2006); 10.1063/1.2213931

An advertisement for Asylum Research Cypher AFMs. The background is dark blue with a film strip graphic on the left. The text is in white and orange. The Oxford Instruments logo is in the bottom right corner.

Not all AFMs are created equal
Asylum Research Cypher™ AFMs
There's no other AFM like Cypher

www.AsylumResearch.com/NoOtherAFMLikeIt

OXFORD
INSTRUMENTS
The Business of Science®

Raman spectra of R_2O_3 (R —rare earth) sesquioxides with C-type bixbyite crystal structure: A comparative study

M. V. Abrashev,^{1,2,a)} N. D. Todorov,² and J. Geshev¹

¹Instituto de Física, UFRGS, Porto Alegre, 91501-970 Rio Grande do Sul, Brazil

²Faculty of Physics, University of Sofia, BG-1164 Sofia, Bulgaria

(Received 10 July 2014; accepted 25 August 2014; published online 9 September 2014)

Raman spectra of R_2O_3 (R —Sc, Er, Y, Ho, Gd, Eu, and Sm) powders with C-type bixbyite crystal structure are measured. With the help of these data and ones, previously published for other oxides from the same structural family, general dependencies of the frequencies of the Raman peaks on the cubic crystal unit cell parameter are constructed. Using these dependencies and knowing the symmetry of the peaks for one of the oxides, determined from previous single-crystal measurements, it is possible to find out the symmetry of the peaks from the spectra of all compounds. It was found that the frequency of the six lowest frequency peaks scales with the square root of the mass of the rare earth showing that mainly R ions take part in these vibrations. These results agree with performed here lattice dynamical calculations. The anomalous softening of the frequency of some peaks in the spectra of Eu_2O_3 is discussed. © 2014 AIP Publishing LLC.

[<http://dx.doi.org/10.1063/1.4894775>]

I. INTRODUCTION

The rare-earth sesquioxides R_2O_3 are promising materials for many technological applications. They are suitable to be used as electroluminescence¹ and cathodoluminescence² sources, catalysts for chemical organic reactions,^{3,4} high- k gate dielectrics,⁵ optical parts of high power lasers,⁶ oxygen ion conducting electrolyte in solid oxide fuel cells,⁷ and materials with strongly hydrophobic surface.⁸ Depending on the type of the rare earth, five different crystal structures are known.⁹ Two of them, the so-called X-phase and H-phase, are stable only above 2000 K.¹⁰ The other three, the hexagonal A-phase, the monoclinic B-phase, and the cubic C-phase, can be observed at ambient conditions. At room temperature, the C-type phase is thermodynamically stable for almost all sesquioxides (those with ionic radius of the rare earth smaller than the one of neodymium). The crystal structure of this phase belongs to the bixbyite-type [of the mineral $(Mn,Fe)_2O_3$]. It can be regarded as an oxygen-deficient superstructure of the simpler CeO_2 (with CaF_2 -type crystal structure) if each fourth oxygen atom from the oxygen chains, parallel to all $\langle 100 \rangle$ crystal directions, is removed^{11,12} (see Fig. 1).

Raman spectroscopy, normally combined with other experimental techniques, can be a useful tool for monitoring the phase content at the stages of synthesis of these compounds and the orientation of single crystals and epitaxially grown thin films, for detection of structural phase transitions changing the temperature or the pressure, or for evaluating the chemical content in the case of solid solutions. For all these purposes, it is necessary to study some general dependencies of the Raman spectra (the frequency, the relative intensity, and the symmetry of the peaks) on the type of the rare earth.

We have thoroughly browsed the existing literature for Raman studies of C-type R_2O_3 oxides. The most informative papers we found, in order of the increasing ionic radius of the rare earth, are for Sc—Refs. 12–18; for Lu—Refs. 17–22; for Tm—Refs. 17, 18, and 23–25; for Er—Refs. 18 and 26–28; for Y—Refs. 11, 14, 15, 17, 18, 22, and 27–29; for Ho—Refs. 15, 18, 25, 28, and 29; for Dy—Refs. 14, 17, 18, 23, 24, 26, 28, and 29; for Tb—Ref. 25; for Gd—Refs. 17, 18, 25, 28, and 30; for Eu—Refs. 14, 17, 18, 24, and 28; for Sm—Refs. 14, 25, 28, 31, and 32; for Nd—Refs. 17 and 25; for Pr—Ref. 25. Although single crystals have been investigated in several studies,^{11,12,15,22,26,27,31} only in few of them^{11,12,27} polarized Raman spectra are shown. In some works, the symmetry of the phonon modes, giving rise to the observed peaks in the Raman spectra of Sc_2O_3 ,^{12,15} Lu_2O_3 ,²² Er_2O_3 ,^{15,26,27} Y_2O_3 ,^{11,15,27} and Dy_2O_3 ,²⁶ has been proposed. However, only for Sc_2O_3 ¹² and to a certain degree for Y_2O_3 ,^{11,15,27} this assignment is supported by the published experimental data. In Refs. 11 and 12, the interpretation of the experimental results has been supported by lattice dynamical calculations (LDCs).

It is natural to expect, for such a large family of isostructural compounds, that some dependencies of their vibrational properties on their structural characteristics to be found. Given that the Raman spectra are dominated by one very intense peak at about 350 cm^{-1} , most of the attempts have been made to find the dependence of the frequency of this peak on the type of the rare earth using as a structural parameter the averaged R -O distance,¹⁴ the number of f -electrons of the R^{3+} ion,^{25,28} or the mass of the R^{3+} ion.¹⁷ It appears that in this case the unit cell parameter of the cubic crystal lattice is the most suitable parameter. It is known with high accuracy for all members of the family. Ubaldini and Carnasciali¹⁷ have found that the frequency of the most intense peak monotonically decreases with the increase of the unit cell parameter. Goueron *et al.*¹⁵ gave such kind of

^{a)}mvabr@phys.uni-sofia.bg

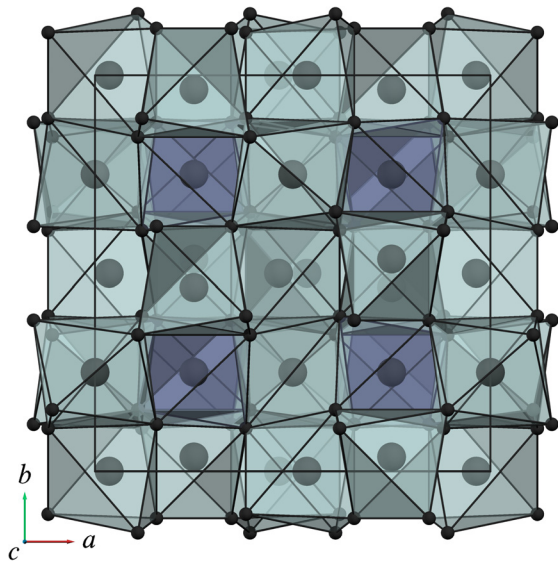


FIG. 1. The crystal structure and the unit cell of C-type R_2O_3 (in the case of $R = \text{Ho}$). The two types of HoO_6 polyhedra are with different shades.

frequency dependencies for six peaks using data of five rare-earth oxides. Urban and Cornilsen,²⁵ however, have stressed that there is a deviation from this dependence in the case of the Eu and Yb oxides.

In this paper, we show a well-pronounced dependence of the frequencies of all most-intense peaks in the Raman spectra of C-type R_2O_3 on the cubic unit cell parameter, based on the data obtained by us for seven oxides as well as on data for other six oxides reported in the literature. Using this dependence and the information concerning the symmetry of the peaks, determined by Sc_2O_3 single crystal measurements,¹² it is easy to determine the symmetry of the corresponding peaks for the rest of the oxides. We also show that in the six modes with lowest frequency mainly R ions take part in the vibrations. The anomalous behavior of the frequency of some peaks in the spectra of Eu_2O_3 is confirmed and discussed.

II. EXPERIMENTAL AND COMPUTATIONAL DETAILS

We studied commercially available (Sigma-Aldrich and Merck) R_2O_3 powders ($R = \text{Sc, Lu, Er, Y, Ho, Gd, Eu, Sm, Nd}$), with purity better than 99.9%, pressed into pellets. The Raman spectra were measured at room temperature in back-scattering geometry using micro-Raman spectrometer LabRAM HR800 Visible. An objective $\times 50$ was used both to focus the incident laser beam onto the pellets surface and to collect the scattered light. The He-Ne (632.8 nm) and Ar^+ (514.5, 488.0, and 457.9 nm) laser lines were used for excitation. No overheating effects were observed at the used laser power of 1.0 mW. Preliminary measurements showed that, due to the transparency of the powder grains (leading to numerous reflections and refractions of the light), the scattered light was completely depolarized, and the Raman spectra in parallel and crossed geometrical configuration of the polarization of the incident and the scattered light were identical. This makes impossible to use the depolarization ratio (the ratio of the intensity of a peak in the crossed and parallel

polarization) of the peaks as a criterion for identifying their symmetry.³³ Therefore, only a non-polarized spectra were measured. As it was mentioned in previous works,^{14,18,29} for some laser lines in addition to the peaks, originating by phonon scattering, in the Raman spectra there are observed other peaks due to fluorescence and/or electronic Raman scattering, originating by transitions between the electronic states of the R^{3+} ions or small impurities of other R^{3+} ions.¹⁸ Their presence might confuse the finding of the corresponding phonon Raman peaks in the different compounds.

At first, we obtained Raman spectra from all the compounds using the available four laser lines. The Raman spectra for Sc_2O_3 and Y_2O_3 , excited with all laser lines, contain only peaks with phononic origin. For Ho_2O_3 , only spectra obtained with 514.5 nm excitation were free from additional peaks. For Er_2O_3 , the optimal excitation is 457.9 nm. For the Lu_2O_3 sample, for all excitations many additional narrow peaks were detected. The spectra of Gd_2O_3 are free from fluorescence peaks. There, however, in addition to the Raman peaks of the C-phase, additional peaks characteristic for the monoclinic B-phase were detected,³⁰ showing that the sample is two-phase. In the case of Sm_2O_3 and Eu_2O_3 the peaks, characteristic for the monoclinic B-phase^{31,32} are dominant. Finally, Nd_2O_3 samples showed Raman spectra of the A-phase.^{34,35} All these observations are in accordance with the expectations about the phase stability for synthesis at standard conditions of the sesquioxides from this family (the phase diagram as a function of the temperature and the type of the rare earth can be found in Refs. 10 and 36). For that reason, in order to obtain single C-type phase samples, the R_2O_3 samples ($R = \text{Sm, Eu, Gd}$) were heated at 500 °C in air for three days and after that heated at 300 °C in air for additional three days. After this procedure, the presence of other phases was almost negligible. Later, Eu_2O_3 was additionally annealed at the same temperatures and time but in oxygen flow (see the discussion below).

We calculated the frequencies of the Γ -point phonons for R_2O_3 ($R = \text{Sc, Y, and Ho}$) in the framework of the shell model as implemented in the Gulp package.³⁷ The ionic polarizability α is taken into account by means of the displacement of massless shell of charge Y from a core, having all of the ion's mass, of charge Z . As the core (representing the nucleus and the inner electrons of the ion) and the shell (representing the valence electrons) are coupled by harmonic spring of force constant k , the ionic polarizability is given by $\alpha = Y^2/k$. The interatomic potentials in this model are represented as a sum of long-range Coulomb potential and short-range potential of the Buckingham form $U_{\text{short-range}} = A \exp(-r/\rho) - C/r^6$. The potentials used for the LDC are presented in Table I. The A parameters for the R ions and the charges were adjusted by a fit to the available crystallographic data, while those for the O-O interaction were taken from Ref. 38.

III. RESULTS AND DISCUSSION

A. General dependencies

The crystal structure of the C-type R_2O_3 oxides has space group $Ia\bar{3}$ ($Z = 16$). The Sc atoms occupy two types of Wyckoff positions, namely, $8b$ and $24d$, whereas all O atoms

TABLE I. Parameters for the short-range interatomic potential. The O^{2-} ions have a core charge of $Y = 1.169|e|$, shell charge of $Z = -3.069|e|$, and force constant $k = 72.94 \text{ eV \AA}^{-2}$. The R^{3+} ions (Sc, Y, and Ho) were treated as a rigid ones, with core charge of $Z = +2.850|e|$.

Ionic pair		A (eV)	ρ (Å)	C (eVÅ ⁶)
Sc core	O shell	1213.1	0.3312	0.000
Y core	O shell	1262.6	0.3491	0.000
Ho core	O shell	1275.2	0.3487	0.000
O shell	O shell	22764.0	0.1490	27.879

occupy the $48e$ position. Although there are 22 Raman-active modes, $4A_g + 4E_g + 14F_g$, the number of the experimentally observed peaks in the Raman spectra is smaller.^{11,12,15} The Raman spectra of the studied samples with single (or dominating) C-type phase are displayed in Fig. 2 where, due to the good signal-to-noise ratio, even the weak peaks can be unambiguously detected. The peaks originating by the minority second monoclinic B-phase in Gd_2O_3 ^{22,30} and Sm_2O_3 ^{31,32} are marked with stars. The two broad bands in the spectrum of Er_2O_3 , probably due to a photoluminescence, are marked with triangles.

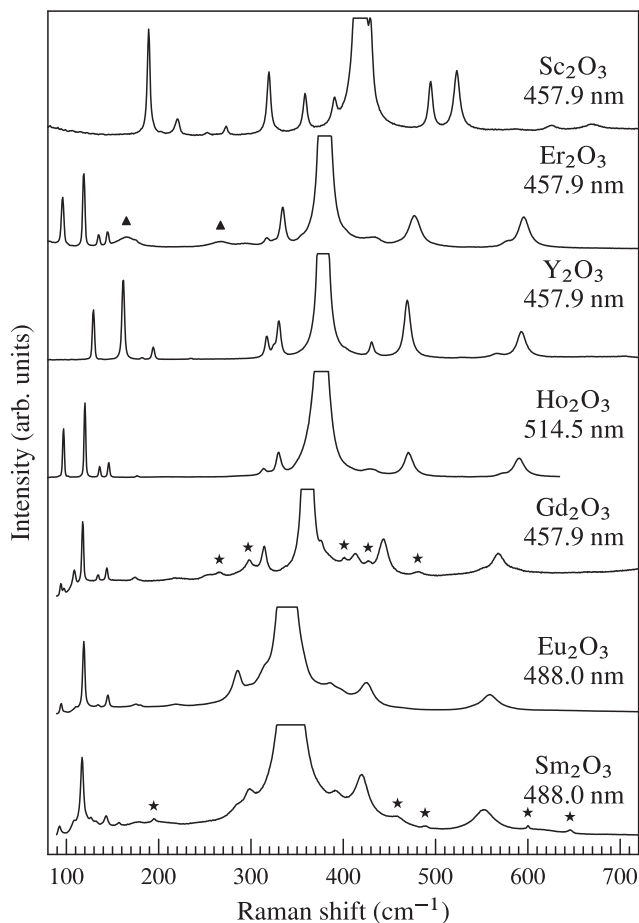


FIG. 2. Raman spectra of R_2O_3 (R —Sc, Er, Y, Ho, Gd, Eu, and Sm) powders. The laser excitation wavelength is indicated for each spectrum. The peaks marked with stars in the spectra of Gd_2O_3 and Sm_2O_3 originate from scattering by phonons in the B-type monoclinic minority phase. The two broad bands marked with triangles in the spectra of Er_2O_3 probably due to a photoluminescence.

The frequencies of the peaks registered for the studied oxides as well as the frequencies for other isostructural R_2O_3 oxides (taken from the literature) are listed in Table II. The most published data coincide in the frame of the typical experimental accuracy for Raman spectra ($\pm 1 \text{ cm}^{-1}$). Note, however, that the data from the highly cited work of White and Keramidas¹⁴ have a systematical shift of about $+12 \text{ cm}^{-1}$, as compared to the other sources.

The dependencies of the most-intense peaks with frequency above 300 cm^{-1} , expected to be predominantly oxygen vibrations, on the unit cell parameter of the corresponding oxides, starting from Sc_2O_3 (the compound with smallest unit cell parameter) up to Pr_2O_3 (the compound with largest unit cell parameter), are shown in Fig. 3. The frequency of all corresponding Raman peaks decreases monotonically with the increase of the cubic unit cell parameter. However, all high-frequency Raman peaks of Eu_2O_3 , marked in Fig. 3 with open symbols, show anomalous “softening” (i.e., they have lower frequency than can be expected from Fig. 3). Up to now, it has been reported only for the most-intense peak at 339 cm^{-1} .²⁵

The symmetry of all corresponding peaks also can be easily found, because in the case of Sc_2O_3 it is unambiguously determined¹² (given in Fig. 3). This assignment is in agreement with those previously done, based on Y_2O_3 single crystal measurements,^{11,15,27} except for the A_g peak at 495 cm^{-1} in Sc_2O_3 (431 cm^{-1} in Y_2O_3). The symmetry of the peak at 359 cm^{-1} is given as $E_g + F_g$ not because of an ambiguity but rather due to the presence of two peaks with different symmetry and coinciding frequencies. The large uncertainty of the determination of the peak symmetry, as shown in Ref. 11, is probably due to the large polarizer leakage seen in the spectra therein.

The comparison of the low-frequency Raman peaks is given in Fig. 4. We remind the simple concept that as in the case of a harmonic oscillator, the frequency of a vibration (phonon mode) briefly is proportional to the square root of the elasticity (or force) constant (the strength of the chemical bond or the type of the environment) and reciprocally proportional to the square root of the mass of vibrating atom (in the more complicated case of a vibration of different types of atoms it is some more complex function of their masses, in particular their reduced mass). Go back to Fig. 4, it is seen that the frequencies of these peaks for the lanthanide oxides (excluding Y_2O_3 and Sc_2O_3) are almost constant. Assuming that these peaks correspond to practically pure lanthanide atoms’ vibrations (as it is confirmed by the LDC), it appears that the effect of the decrease of the mass of the lanthanide, leading to the increase of the mode frequency, is fully compensated by the effect of the increase of the unit cell parameter (or the R -O distance, or the ionic R^{3+} radius), leading to the decrease of the mode frequency. A similar constant mode frequency was observed for a R -mode in the family R_2CuO_4 (R —Pr, Nd, Sm, Gd).⁴⁹

To check which are the corresponding pure yttrium phonon modes in Y_2O_3 , it is necessary to compare their frequencies with the ones for the lanthanide oxide with the closest unit cell parameter (or closest ionic radius, i.e., Ho) and to correct (normalize) its frequencies, accounting for the very

TABLE II. Frequencies of the most-intense peaks in the Raman spectra of some C-type R_2O_3 . The symmetry of the peaks, as determined by Sc_2O_3 single crystal measurements,¹² is listed on the first row. In the bottom of the table, there are earlier assignments given based on Y_2O_3 single crystal measurements.^{11,15,27}

R	a (Å)	Reference structure	F_g	F_g	A_g	F_g	$E_g + F_g$	F_g	E_g	F_g	A_g	F_g	F_g	Reference Raman
Sc	9.830	12	669	523	495	419	359	319	273	252	221	202	189	This work
Lu	10.391	39	612	499	454	393	348		146	137	120		98	21, 22
Tm	10.491	40	604	485	438	384	334		144	136	121		97	23, 24
Er	10.561	41	595	478	434	379	334	175	144	135	119		97	This work
Y	10.602	42	592	469	431	377	325	235	194	182	162	138	129	This work
Ho	10.617	43	590	471	430	376	330	176	146	136	120	102	97	This work
Dy	10.668	41	589	464	425	371	330		145	136	120		96	23, 24
Tb	10.729	44		450							118		95	25
Gd	10.817	45	569	444	414	361	315	175	145	135	119	110	95	This work
Eu	10.868	46	559	425	385	339	289	175	145	134	119	109	94	This work
Sm	10.930	47	554	421	393	345	299	179	144	133	118	109	94	This work
Nd	11.072	48	539	401							116		100	17, 25
Pr	11.152	9		393							117		99	25
			$F_g + A_g$	$F_g + A_g$	$F_g + E_g$	$F_g + A_g$	$E_g + F_g$	F_g	$F_g + E_g$	F_g	$F_g + A_g$		F_g	11
			F_g	F_g	F_g	F_g	E_g		E_g	F_g	$F_g + A_g$		F_g	15
			F_g	F_g	F_g	$F_g + A_g$	E_g			F_g	$F_g + A_g$		F_g	27

different mass of Y compared to the one of Ho. Therefore, in Fig. 4, the frequencies of the peaks from the spectra of Y_2O_3 and Sc_2O_3 are normalized to be easily compared to the

frequencies of the peaks of the other lanthanide compounds, multiplying them by $\sqrt{m_Y/m_{Ho}}$ and $\sqrt{m_{Sc}/m_{Ho}}$, respectively. It is seen that the thus-normalized frequencies for Y_2O_3 are very close to those of Ho_2O_3 , proving the pure lanthanide origin of these vibrations (i.e., it is observed pure “isotope” effect). Even in the case of Sc_2O_3 , despite the large difference between its unit cell parameter and those of the other compounds, the normalized frequencies still have such a value, so the corresponding peaks can be identified. So, the symmetry of these peaks for all lanthanide compounds can

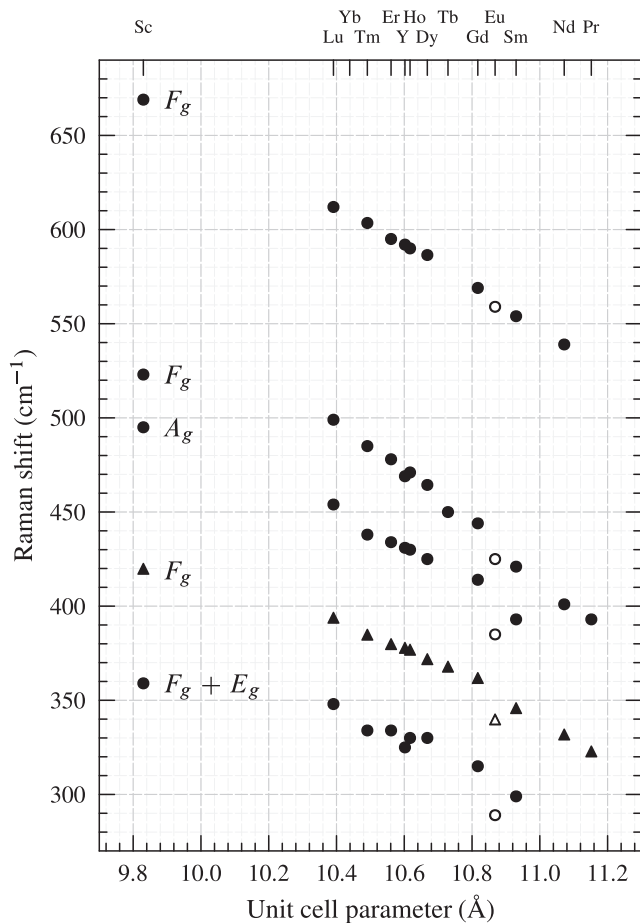


FIG. 3. Dependencies of the frequency of the high-frequency Raman peaks on the cubic unit cell parameter of the C-type crystal structure. The symmetry of the peaks, as determined from Sc_2O_3 single crystal measurements,¹² is indicated. The peak with an order larger intensity than the others is indicated by a triangle.

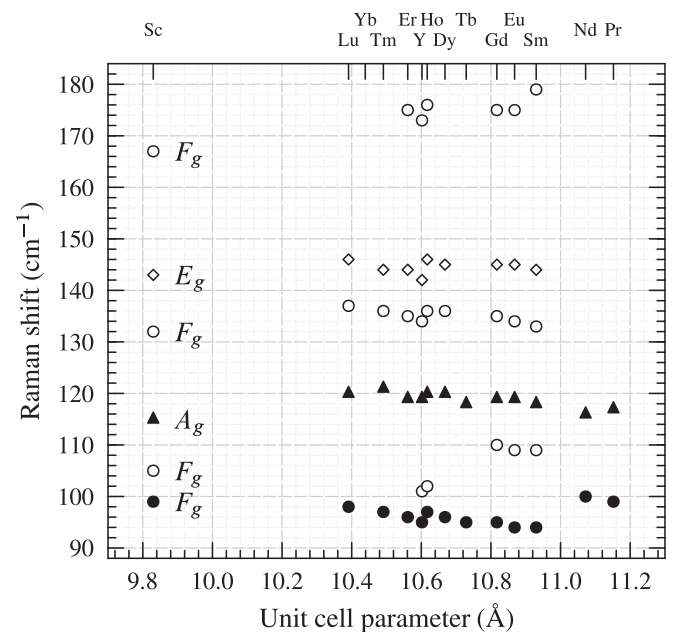


FIG. 4. Dependencies of the frequency of the low-frequency Raman peaks on the cubic unit cell parameter of the C-type crystal structure. For better comparison, the frequency of the peaks from the spectra of Y_2O_3 and Sc_2O_3 is normalized to the frequency of the peaks of the other compounds (Ho_2O_3) multiplying it by $\sqrt{m_Y/m_{Ho}}$ and $\sqrt{m_{Sc}/m_{Ho}}$, respectively. The symmetry of the peaks, as determined by Sc_2O_3 single crystal measurements,¹² is indicated. The filled symbols correspond to the peaks with higher intensity.

be determined using this correspondence, and the known symmetry of the Sc_2O_3 peaks, obtained by single crystal measurements.¹²

A comparison between the experimental and calculated Raman-active mode frequencies is shown in Table III. As it is seen, the low-frequency modes obtained from the LDC are in a good agreement with the experiment. As it is noted already above, the calculations confirm that in these vibrations mainly R ions take part.

B. Anomalous behavior of Eu_2O_3

Comparing the data from Figs. 3 and 4, it can be noted that, contrary to the high-frequency modes of Eu_2O_3 , its low-frequency modes do not show any anomalous decrease of the frequency (“softening”). The frequencies of the Eu_2O_3 low-frequency modes are practically the same as those of their neighbors by unit cell parameter, Gd_2O_3 and Sm_2O_3 (see Fig. 4). Trying to understand the reason for the anomalous lower values of the frequencies of the Eu_2O_3 high-frequency Raman peaks, we construct the dependence of the relative softening $-(\omega_{\text{expt}} - \omega_{\text{dep}})/\omega_{\text{dep}}$ on ω_{dep} . Here, ω_{expt} is the experimentally observed frequency and ω_{dep} for Eu_2O_3 is obtained using linear interpolation of the frequencies for its nearest neighbors by unit cell parameter Gd_2O_3 and Sm_2O_3 . The so-constructed dependence is given in Fig. 5.

It is seen that the anomaly (the “softening”) is maximal for the modes with frequencies ranging from 300 to 400 cm^{-1} (pure oxygen modes). For ionic oxides usually in this frequency region are the oxygen bending (in respect to metal-oxygen bonds) modes. These observations do not favor the previously proposed explanation for the origin of

TABLE III. Experimental (for Sc_2O_3 —this paper and Ref. 12) and calculated frequencies of the Raman-active modes in $R_2\text{O}_3$ (R —Sc, Y, and Ho).

Symmetry	Sc_2O_3		Y_2O_3		Ho_2O_3	
	ω_{expt}	ω_{calc}	ω_{expt}	ω_{calc}	ω_{expt}	ω_{calc}
F_g	189	192	129	132	97	98
	202	199	138	138	102	103
	252	250	182	181	136	136
	319	306	235	234	176	179
	329	311		244		184
	359	341	325	288	330	287
		368		299		291
	391	386		338		334
	419	412	377	368	376	364
		472		416		409
		491		442		438
		523	536	469	495	471
E_g	587	605		545		536
	669	646	592	581	590	574
	273	273	194	198	146	149
	359	332	325	290	330	287
	430	416		366		361
	626	590		555		555
A_g	221	220	162	162	120	123
	391	351		306		297
	495	498	431	460	430	459
	623	593		553		553

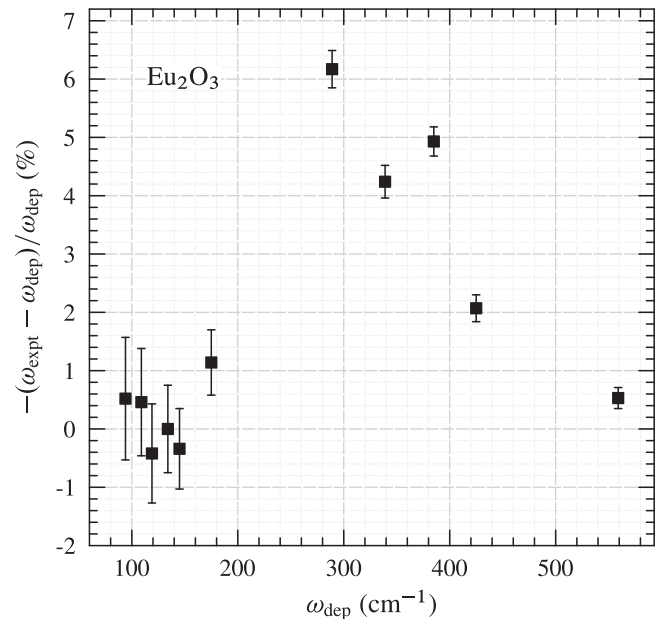


FIG. 5. The softening (in %) of the frequency of the phonon modes in Eu_2O_3 as a function of their expected frequency ω_{dep} (if it follows the general dependence).

the anomalous mode frequency—the specific Eu^{3+} electronic structure.²⁵ Note that just the low-frequency Eu vibrations are not influenced. So, the reason for the anomaly could be in some peculiarities of the oxygen sublattice. Using lattice dynamical calculations, Todorov *et al.*¹² have determined the origin of the most-intensive Raman-active F_g peak (in the case of Sc_2O_3 at 419 cm^{-1} , corresponding to the 339 cm^{-1} peak for Eu_2O_3) as oxygen vibrations along the oxygen chains, parallel to the $\langle 100 \rangle$ crystal directions. Due to the nature of this mode (the directions of the oxygen vibration) the frequency of this mode depends most on the oxygen-oxygen interaction. The LDCs for Y_2O_3 and Ho_2O_3 presented here show the same vibrational pattern for the corresponding peaks at 377 and 376 cm^{-1} (calculated at 368 and 364 cm^{-1}), respectively. According to the LDC, the other modes in this middle-frequency region have similar vibrational (bending-type) origin. It is natural to expect that this type of modes are most sensitive to a presence of oxygen vacancies in the crystal structure of Eu_2O_3 . Therefore, a small oxygen deficiency is the probable reason for the anomalous softening of the oxygen modes in Eu_2O_3 .

For several oxides with variable oxygen content, it is known that the frequencies of some oxygen vibrations in them are very sensitive to their oxygen content (non-stoichiometry).^{50,51} Usually, a change of the oxygen content causes noticeable modifications of the structural data. However, examining the structural data for the $R_2\text{O}_3$ oxides, we did not find any anomaly neither for the unit cell parameter nor for the partial atomic coordinates of the oxygen ions in the unit cell of Eu_2O_3 . In order to increase the oxygen content in Eu_2O_3 , we made an attempt to remove the hypothetical oxygen vacancies by additionally annealing the samples first at 500°C and after that at 300°C , both in flowing oxygen for three days. However, the increase of the frequency of the most-intense peak was (if any) less than 0.5 cm^{-1} .

Nevertheless, we believe that the problem concerning the anomalous phonon dynamics of Eu_2O_3 remains open and needs additional study of structurally well-characterized samples annealed in oxygen at different (high) pressures. This interest is reinforced by some recent publications reporting a detection, via X-ray photoelectron spectroscopy, of oxygen vacancies in Eu_2O_3 samples.^{52,53}

IV. CONCLUSIONS

A complete comparative study of the Raman-active phonon modes in the $R_2\text{O}_3$ (R —rare earth) oxides with C-type bixbyite crystal structure was reported. The optimal conditions (the choice of the laser line and additional temperature annealing of the samples) for measuring of the Raman spectra, containing only one-phonon Raman peaks, without additional peaks due to photoluminescence, electronic Raman scattering, or secondary minority monoclinic B-phase, were studied. The results of the measurements of seven oxides as well the previously published results for other six oxides were compared. It appears that due to the large difference of the mass of the oxygen and rare earth ions, the phonon modes can be separated into two groups—high-frequency pure oxygen vibrations and low-frequency pure rare-earth vibrations. The frequency of the high-frequency oxygen modes shows smooth and clear dependence on the type of the oxide, as it is monotonously decreases with the increase of the cubic unit cell parameter of the oxide. In opposite, the practically constant frequency of the corresponding low-frequency rare-earth modes in the different lanthanide oxides shows that the effects of the change of the lanthanide mass and the change of the unit cell parameters compensate each other. The LDC shows good agreement between the calculated and experimentally observed phonon frequencies as well confirm the origin of the phonon modes. In the case of Eu_2O_3 , it was observed systematic lower frequency (“softening”) for the middle-frequency oxygen vibrations compared to the expected ones from the general dependencies. Analyzing these results, we suggest that the reason for this anomaly is the presence of oxygen vacancies (non-stoichiometry) in its crystal structure. Unfortunately, annealing the samples in flowing oxygen did not change the Raman spectra. The Eu_2O_3 anomaly needs additional detailed investigation.

ACKNOWLEDGMENTS

M.V.A. thanks the Brazilian agency CAPES (Project No. BEX 7607-13-0). N.D.T. acknowledges the Science Fund of the University of Sofia, Bulgaria (Contract No. 085/2014). This work has also been supported by the Brazilian agency CNPq (Project No. 483277/2012-6).

¹A. H. Kitai, *Thin Solid Films* **445**, 367 (2003).

²E. W. Barrera, M. C. Pujol, F. Diaz, S. B. Choi, F. Rotermund, K. H. Park, M. S. Jeong, and C. Cascales, *Nanotechnology* **22**, 075205 (2011).

³A. G. Dedov, A. S. Loktev, I. I. Moiseev, A. Aboukais, J.-F. Lamonier, and I. N. Filimonov, *Appl. Catal., A* **245**, 209 (2003).

⁴D. Andreeva, I. Ivanov, L. Ilieva, M. V. Abrashev, R. Zanella, J. W. Sobczak, W. Lisowski, M. Kantcheva, G. Avdeev, and K. Petrov, *Appl. Catal., A* **357**, 159 (2009).

⁵T.-M. Pan and W.-S. Huang, *Appl. Surf. Sci.* **255**, 4979 (2009).

⁶D. E. Zelmon, J. M. Nothridge, N. D. Haynes, D. Petrov, and K. Petermann, *Appl. Opt.* **52**, 3824 (2013).

⁷N. Orlovskaya, S. Lukich, G. Subhash, T. Graule, and J. Kuebler, *J. Power Sources* **195**, 2774 (2010).

⁸G. Azimi, R. Dhiman, H.-M. Kwon, A. T. Paxson, and K. K. Varanasi, *Nat. Mater.* **12**, 315 (2013).

⁹G. Adachi and N. Imanaka, *Chem. Rev.* **98**, 1479 (1998).

¹⁰M. Zinkevich, *Prog. Mater. Sci.* **52**, 597 (2007).

¹¹Y. Repelin, C. Proust, E. Husson, and J. M. Beny, *J. Solid State Chem.* **118**, 163 (1995).

¹²N. D. Todorov, M. V. Abrashev, V. Marinova, M. Kadiyski, L. Dimowa, and E. Faulques, *Phys. Rev. B* **87**, 104301 (2013).

¹³D. Liu, W. Lei, Y. Ma, J. Hao, X. Chen, Y. Jin, D. Liu, S. Yu, Q. Cui, and G. Zou, *Inorg. Chem.* **48**, 8251 (2009).

¹⁴W. B. White and V. G. Keramidis, *Spectrochim. Acta, Part A* **28**, 501 (1972).

¹⁵J. Gouteron, J. Zarembowitch, and A.-M. Lejus, *C. R. Acad. Sci.* **289**, 243 (1979); available at http://apps.webofknowledge.com/full_record.do?product=UA&search_mode=GeneralSearch&qid=1&SID=2Cvpc9jBE18cu2noTH&page=1&doc=3&cacheurlFromRightClick=no

¹⁶A. A. Kaminskii, S. N. Bagaev, K. Ueda, K. Takaichi, J. Li, A. Shirakawa, H. Yagi, T. Yanagitani, H. J. Eichler, and H. Rhee, *Laser Phys. Lett.* **2**, 30 (2005).

¹⁷A. Ubaldini and M. M. Carnasciali, *J. Alloys Compd.* **454**, 374 (2008).

¹⁸J. Yu, L. Cui, H. He, Sh. Yan, Y. Hu, and H. Wu, *J. Rare Earths* **32**, 1 (2014).

¹⁹C.-M. Lin, K.-T. Wu, T.-L. Hung, H.-S. Sheu, M.-H. Tsai, J.-F. Lee, and J.-J. Lee, *Solid State Commun.* **150**, 1564 (2010).

²⁰V. Grover, A. Banerji, P. Sengupta, and A. K. Tyagi, *J. Solid State Chem.* **181**, 1930 (2008).

²¹A. Garcia-Murillo, C. Le Luyer, C. Pedrini, and J. Mugnier, *J. Alloys Compd.* **323–324**, 74 (2001).

²²L. Laversenne, Y. Guyot, C. Goutaudier, M. Th. Cohen-Adad, and G. Boulon, *Opt. Mater.* **16**, 475 (2001).

²³X. Fu, Y. Xu, and J. Zhou, *J. Mater. Sci.* **47**, 1697 (2012).

²⁴L. A. Tucker, F. J. Carney, Jr., P. McMillan, S. H. Lin, and L. Eyring, *Appl. Spectrosc.* **38**, 857 (1984).

²⁵M. W. Urban and B. C. Cornilsen, *J. Phys. Chem. Solids* **48**, 475 (1987).

²⁶J. B. Gruber, R. D. Chirico, and E. F. Westrum, Jr., *J. Chem. Phys.* **76**, 4600 (1982).

²⁷G. Schaack and J. A. Koningstein, *J. Opt. Soc. Am.* **60**, 1110 (1970).

²⁸N. Dilawar, S. Mehrotra, D. Varandani, B. V. Kumaraswamy, S. K. Haldar, and A. K. Bandyopadhyay, *Mater. Charact.* **59**, 462 (2008).

²⁹J.-C. Panitz, J.-C. Mayor, B. Grob, and W. Durisch, *J. Alloys Compd.* **303–304**, 340 (2000).

³⁰P. Mele, C. Artini, A. Ubaldini, G. A. Costa, M. M. Carnasciali, and R. Masini, *J. Phys. Chem. Solids* **70**, 276 (2009).

³¹J.-F. Martel, S. Jandl, A. M. Lejus, B. Viana, and D. Vivien, *J. Alloys Compd.* **275–277**, 353 (1998).

³²S. Jiang, J. Liu, C. Lin, X. Li, and Y. Li, *J. Appl. Phys.* **113**, 113502 (2013).

³³G. Herzberg, *Molecular Spectra and Molecular Structure* (Van Nostrand Reinhold Company, New York, 1945), Vol. II, p. 245.

³⁴S. I. Boldish and W. B. White, *Spectrochim. Acta, Part A* **35**, 1235 (1979).

³⁵S. Jandle, J.-P. Rheault, and M. Poirier, *Phys. Rev. B* **56**, 11600 (1997).

³⁶P. P. Fedorov, M. V. Nazarkin, and R. M. Zakalyukin, *Crystallogr. Rep.* **47**, 281 (2002).

³⁷G. D. Gale, *J. Chem. Soc., Faraday Trans.* **93**, 629 (1997).

³⁸G. V. Lewis and C. R. A. Catlow, *J. Phys. C: Solid State Phys.* **18**, 1149 (1985).

³⁹L. Ben Farhat, M. Amami, E. K. Hilal, and R. Ben Hassen, *Mater. Chem. Phys.* **123**, 737 (2010).

⁴⁰J. Blanus, M. Mitric, D. Rodic, A. Szytula, and M. Slaski, *J. Magn. Magn. Mater.* **213**, 75 (2000).

⁴¹Z. K. Heiba, M. Bakr Mohamed, M. A. Abdelslam, and L. H. Fuess, *Cryst. Res. Technol.* **46**, 272 (2011).

⁴²M. Mitric, A. Kremenovic, R. Dimitrijevic, and D. Rodic, *Solid State Ionics* **101–103**, 495 (1997).

⁴³Z. K. Heiba, M. Bakr Mohamed, and H. Fuess, *Cryst. Res. Technol.* **47**, 535 (2012).

⁴⁴A. Saiki, N. Ishizawa, N. Mizutani, and M. Kato, *J. Ceram. Soc. Jpn.* **93**, 649 (1985); available at <http://www.scopus.com/record/display.url?eid=2-s2.0-0022207174&origin=resultslist&sort=plf-f&src=s&st1=Ishizawa+N&>

- st2=Mizutani+N&sid=8D2B089096F39BEF673C03D33D1DDA75.kqQeWtawXauCyC8ghhRGJg%3a20&sot=b&sdt=b&sl=53&s=%28AUTHOR-NAME%28Ishizawa+N%29+AND+AUTHOR-NAME%28Mizutani+N%29%29&relpos=18&relpos=18&citeCnt=41&searchTerm=%28AUTHOR-NAME%28Ishizawa+N%29+AND+AUTHOR-NAME%28Mizutani+N%29%29
- ⁴⁵B. J. Kennedy and M. Avdeev, *Aust. J. Chem.* **64**, 119 (2011).
- ⁴⁶Z. K. Heiba, Y. Akin, W. Sigmund, and Y. S. Hascicek, *J. Appl. Crystallogr.* **36**, 1411 (2003).
- ⁴⁷M. Mitric, J. Blanusa, T. Barudzija, Z. Jaglicic, V. Kusigerski, and V. Spasojevic, *J. Alloys Compd.* **485**, 473 (2009).
- ⁴⁸H. Bommer, *Z. Anorg. Allg. Chem.* **241**, 273 (1939).
- ⁴⁹M. Udagawa, Y. Nagaoka, N. Ogita, M. Masada, and J. Akimitsu, *Phys. Rev. B* **49**, 585 (1994).
- ⁵⁰O. V. Misochko, S. Tajima, S. Miyamoto, H. Kobayashi, S. Kagiya, N. Watanabe, N. Koshizuka, and S. Tanaka, *Phys. Rev. B* **51**, 1346 (1995).
- ⁵¹M. V. Abrashev, M. N. Iliev, and L. N. Bozukov, *Physica C* **200**, 189 (1992).
- ⁵²P. Zngang, Y. Zhao, T. Zhai, X. Lu, Zh. Liu, F. Xiao, P. Liu, and Y. Tong, *J. Electrochem. Soc.* **159**, D204 (2012).
- ⁵³T. Zhang, X. Ou, W. Zhang, J. Yin, Y. Xia, and Zh. Liu, *J. Phys. D: Appl. Phys.* **47**, 065302 (2014).